

FREE VIBRATION OF MOVING LAMINATED COMPOSITE PLATES WITH AND WITHOUT SKEW ROLLER USING THE ELEMENT-FREE GALERKIN METHOD*

E. JABERZADEH, M. AZHARI ** AND B. BOROOMAND

Dept. of Civil Engineering, Isfahan University of Technology, 84156-83111, Isfahan, Iran
Email: mojtaba@cc.iut.ac.ir

Abstract– In this paper, free vibration of axially moving symmetrically laminated plates subjected to in-plan forces is analyzed using the element-free Galerkin method. This category includes symmetric cross-ply and angle-ply laminates and anisotropic plates. The governing differential equation for a moving plate is numerically solved using the Galerkin method. The shape functions are constructed using the moving least squares (MLS) approximation and the essential boundary conditions are introduced into the formulation through the use of the Lagrange multiplier method and the orthogonal transformation techniques. The effect of skew roller and intermediate supports on the natural frequency of plate are examined.

Keywords– Moving plate, element-free Galerkin method, laminated composite plate, skew roller, intermediate supports

1. INTRODUCTION

Axially moving systems are applicable in a wide range of engineering problems which arise in industrial, civil, aerospace, mechanical, electronic and automotive applications. Some specific examples are papers, plastics and composites in production lines, power transmission and conveyor belts, the paper and plastic sheets in the process, the steel strip in a thin steel sheet production line, the band saw blade, etc. In many of these instances, the moving material is not isotropic, but is a single-layer orthotropic material or consists of several orthotropic layers [1].

The axial speed greatly affects the dynamic behavior of the system even at low speeds. Therefore, it becomes a serious problem in achieving good quality for produced materials. In a certain critical velocity, the first natural frequency of the system becomes zero and the straight configuration of equilibrium becomes unstable. Thus, accurate prediction of dynamic characteristics of such structures is required for the analysis and optimal design of a broad class of technological devices [2].

The wide interest in vibrations of axially moving systems has given rise to large scientific productions. The first studies on the subject date back to the last century, Ashley and Haviland studied the bending vibration of a pipe line containing flowing fluid [3].

Many of the previous studies for axially moving continua used one-dimensional string or beam theory instead of plate theory. Swope and Ames studied the vibrations of finite and infinite moving threadlines. Their paper qualitatively described the effect of the axial velocity on the linear frequencies [4]. Mote computed band saw flexural natural frequencies using the Euler–Bernoulli beam theory [5]. The effects of longitudinal steady translational motion on the vibration frequencies and modes of simple Euler beams were considered by Simpson [6].

*Received by the editors March 17, 2013; Accepted November 26, 2013.

**Corresponding author

Although one-dimensional models lead to reliable results for narrow isotropic strips, two-dimensional analysis is required for modeling of many problems such as composite materials, wide width plates, non-uniform forces across the width, no free lateral boundaries, intermediate supports, etc. Ulsoy and Mote [7] proposed a two-dimensional plate modeling of a wide band saw blade. In 1995, Lin and Mote [8] examined the equilibrium displacement and stress distribution of the web with small flexural stiffness under transverse loading. Lengoc and Mccalion [9] considered cutting conditions on dynamic response of bandsaw blades. Afterwards, Lin [10] investigated the stability and vibration characteristics of two-dimensional axially moving plates with two simply supported and two free edges, subjected to uniform in-plane tension in the transport direction.

Using the finite element method, Wang [11] and Laukkanen [12] presented the numerical analysis of the moving thin plates. Their works were based on the mixed interpolated tensorial component plate bending elements and four-node Mindlin–Reisser-type bending elements, respectively. Luo and Hutton [13] presented the formulation of a moving triangular isotropic plate element subjected to in-plane forces and gyroscopic forces and compared the results with the Rayleigh–Ritz method.

More recently, free vibration of moving laminated composite plates was studied by Hatami et al, using an exact and a semi-analytical finite strip method [1]. They found that the translating speed, boundary conditions and the aspect ratio have effects on the natural frequencies of a moving plate. Their research included only straight rollers. They also introduced an exact finite strip method to analyze moving viscoelastic plates [14]. Wang et al. carried out a dynamic analysis of an axially translating plate with time-variant length [15].

In recent years, a class of new numerical method called mesh-free or mesh-less method has been developed and successfully applied in solid mechanics. Mesh-less methods have been extensively used for solving problems in applied mechanics [16-18].

Different versions of mesh-free method have been proposed, such as smooth particle hydrodynamics (SPH) [19], mesh-less local Petrov-Galerkin (MLPG) method [20], finite point method (FPM) [21-23] and element-free Galerkin (EFG) method [24, 25]. The EFG method is a well-developed method that uses the moving least squares (MLS) approach for field approximation. The EFG formulation does not require element connectivity among the nodes and only a set of nodes scattered in the problem domain is used. This makes the EFG method simpler than the finite element method (FEM) in domain discretization procedure. An important aspect is that EFG can treat plates and shells with C^1 -continuity if at least complete quadratic polynomial basis is used [26].

The EFG method has so far been applied to many problems in solids and structures, such as deflection analysis of thin plates [27] and shells [28], vibration of thin plates and analysis of laminated plates [29, 30]. In this method, the generalized displacement at an arbitrary point is approximated from nodal displacements using the moving least squares (MLS) approximation. A domain of compact support is predetermined and only nodes within the domain are included in the interpolation.

In the present work, the EFG is applied to study the transverse vibration of axially moving symmetrically laminated composite plates. The category of symmetrically laminated plates may include cross-ply or angle-ply laminates and may have orthotropic or anisotropic bending properties. The effect of skew-end roller on the natural frequency of axially moving laminates is investigated. It can be easily modeled by the EFG. In the present formulations, the deflection of plates is the only unknown at a node. Therefore, the dimension of the discrete eigenvalue equations obtained by the present formulation is equal to the number of nodes that discretize the plate domain.

This paper is organized into the following sections. In Section 2, the element-free Galerkin method is overviewed. In Section 3, mathematical formulation of the problem for axially moving plates is presented. Plate properties and boundary conditions are mentioned in Section 4, and then, numerical results and discussions are demonstrated in Section 5. Finally, some concluding remarks are presented in Section 6.

2. ELEMENT-FREE GALERKIN METHOD

a) MLS approximants

The EFG employs the moving least-squares (MLS) to generate the shape functions for $w^h(\mathbf{x})$ as an approximation of the real displacement $w(\mathbf{x})$. The weak form of the Galerkin method is used to develop the discretized system of equations.

Moving least squares (MLS) method is now widely used in construction of shape functions for the mesh-free method. Its general formulation is briefly given here. In this method the displacement of a point of interest \mathbf{x} , say $w(\mathbf{x})$, is approximated with a displacement approximation function $w^h(\mathbf{x})$ in the following form

$$w^h(\mathbf{x}) = \sum_{j=1}^m p_j(\mathbf{x}) a_j(\mathbf{x}) \equiv \mathbf{p}^T(\mathbf{x}) \mathbf{a}(\mathbf{x}) \quad (1)$$

where $\mathbf{p}(\mathbf{x})$ is a complete basis whose components are monomials in terms of the coordinates. In this paper, the polynomial basis is chosen as

$$\mathbf{p}^T(\mathbf{x}) = \{1, x, y, x^2, xy, y^2\} \quad m = 6 \quad (2)$$

in which m is the number of bases.

The coefficients $\mathbf{a}(\mathbf{x})$ are functions of \mathbf{x} , and are represented as

$$\mathbf{a}(\mathbf{x}) = \{a_1(\mathbf{x}), a_2(\mathbf{x}), \dots, a_m(\mathbf{x})\} \quad (3)$$

These coefficients are obtained at any point \mathbf{x} by minimizing a functional of weighted residual as follows

$$J = \sum_{I=1}^{Nod} \tilde{w}(\mathbf{x} - \mathbf{x}_I) [w^h(\mathbf{x} - \mathbf{x}_I) - w(\mathbf{x}_I)]^2 = \sum_{I=1}^n \tilde{w}(\mathbf{x} - \mathbf{x}_I) [\mathbf{p}^T(\mathbf{x}_I) \mathbf{a}(\mathbf{x}) - w_I]^2 \quad (4)$$

where Nod is the number of nodes in the neighborhood of \mathbf{x} , which is also called the influence domain of \mathbf{x} . Also, $\tilde{w}(\mathbf{x} - \mathbf{x}_I)$ is a weight function and w_I is the nodal parameter at node I . At an arbitrary point \mathbf{x} , $\mathbf{a}(\mathbf{x})$ is determined so that

$$\frac{\partial J}{\partial \mathbf{a}} = 0 \quad (5)$$

which results in the following linear equation system:

$$\mathbf{A}(\mathbf{x}) \mathbf{a}(\mathbf{x}) = \mathbf{B}(\mathbf{x}) \mathbf{w} \quad (6)$$

where the symmetric matrix \mathbf{A} is called weighted moment and \mathbf{B} is a non-symmetric matrix in the form of

$$\mathbf{A}(\mathbf{x}) = \sum_{I=1}^{Nod} \tilde{w}(\mathbf{x} - \mathbf{x}_I) \mathbf{p}(\mathbf{x}_I) \mathbf{p}^T(\mathbf{x}_I) \quad (7)$$

$$\mathbf{B}(\mathbf{x}) = \{\tilde{w}(\mathbf{x} - \mathbf{x}_I) \mathbf{p}(\mathbf{x}_I), \dots, \tilde{w}(\mathbf{x} - \mathbf{x}_n) \mathbf{p}(\mathbf{x}_n)\} \quad (8)$$

Substituting Eq. (6) into Eq. (4), leads to

$$w^h(\mathbf{x}) = \sum_{I=1}^{Nod} \mathbf{p}^T(\mathbf{x}) \mathbf{A}^{-1}(\mathbf{x}) \mathbf{B}(\mathbf{x}) w_I = \sum_{I=1}^{Nod} \Phi_I(\mathbf{x}) w_I \quad (9)$$

In order to establish the eigenvalue equation of a free vibration problem, the first and second order partial derivatives of the shape function $\Phi_I(\mathbf{x})$ need to be computed. To efficiently compute these partial derivatives, we define

$$\boldsymbol{\gamma}(\mathbf{x}) = \mathbf{A}^{-1}(\mathbf{x}) \mathbf{p}(\mathbf{x}) \quad (10)$$

Hence, we have

$$\boldsymbol{\Phi}(\mathbf{x}) = \boldsymbol{\gamma}^T(\mathbf{x}) \mathbf{B}(\mathbf{x}) \quad (11)$$

and

$$\mathbf{A} \boldsymbol{\gamma} = \mathbf{p} \quad (12)$$

The partial derivatives of $\gamma(\mathbf{x})$ can be obtained by

$$\mathbf{A}\gamma_{,i} = \mathbf{p}_{,i} - \mathbf{A}_{,i}\gamma \quad (13)$$

or

$$\mathbf{A}\gamma_{,ij} = \mathbf{p}_{,ij} - (\mathbf{A}_{,i}\gamma_{,j} + \mathbf{A}_{,j}\gamma_{,i} + \mathbf{A}_{,ij}\gamma) \quad (14)$$

In Eq. (13) and (14) the partial differentiations with respect to x and y are represented by the comma-subscript convention. The partial derivatives of shape function Φ can be obtained as follows:

$$\Phi_{,i} = \gamma^{T}_{,i}(\mathbf{x})\mathbf{B}(\mathbf{x}) + \gamma^T(\mathbf{x})\mathbf{B}_{,i}(\mathbf{x}) \quad (15)$$

or

$$\Phi_{,ij} = \gamma^{T}_{,ij}\mathbf{B} + \gamma^T_{,i}\mathbf{B}_{,j} + \gamma^T_{,j}\mathbf{B}_{,i} + \gamma^T\mathbf{B}_{,ij} \quad (16)$$

b) Weight functions

The choice of the weight function is very important and affects the performance of the EFG method. The weight function controls the influence domain of a point. Several weight functions are available in literature [31]. Here, the well-known quadratic spline is employed which provides continuity in the first and second derivatives.

$$\tilde{w}(\mathbf{x}-\mathbf{x}_I) = \tilde{w}_I(r) = \begin{cases} 1 - 6r^2 + 8r^3 - 3r^4 & r \leq 1 \\ 0 & r > 1 \end{cases} \quad (17)$$

The normalized distance is

$$r = \frac{\|\mathbf{x} - \mathbf{x}_I\|}{\tilde{R}_I} \quad (18)$$

where \tilde{R}_I is the size of the influence domain. This parameter should be chosen in such a way that the matrix \mathbf{A} becomes regular, i.e. the domain of influence of each node must have enough neighborhood nodes to make \mathbf{A} invertible.

3. MATHEMATICAL FORMULATION OF THE PROBLEM FOR AN AXIALLY MOVING PLATE

a) Differential equation and material properties

The governing differential equation for an axially moving laminated plate subjected to plane stress is expressed as

$$\begin{aligned} D_{11} \frac{\partial^4 w}{\partial x^4} + D_{22} \frac{\partial^4 w}{\partial y^4} + 4D_{16} \frac{\partial^4 w}{\partial x^3 \partial y} + 4D_{26} \frac{\partial^4 w}{\partial x \partial y^3} + 2(D_{12} + 2D_{66}) \frac{\partial^4 w}{\partial x^2 \partial y^2} \\ - (N_x \frac{\partial^2 w}{\partial x^2} + 2N_{xy} \frac{\partial^2 w}{\partial x \partial y} + N_y \frac{\partial^2 w}{\partial y^2}) + \rho h (\frac{\partial^2 w}{\partial t^2} + 2v \frac{\partial^2 w}{\partial x \partial t} + v^2 \frac{\partial^2 w}{\partial x^2}) = 0 \end{aligned} \quad (19)$$

where ρ is the average mass per volume of the laminate. N_x and N_y are the in-plane forces per unit length in x and y directions, respectively. N_{xy} is the shear in-plane force per unit length and v is the constant velocity of plate in longitudinal direction of plate. Here the stiffness coefficients D_{ij} for a laminate consisting of nl orthotropic layers and total thickness h are defined as [1]

$$D_{ij} = \int_{-h/2}^{h/2} \bar{Q}_{ij} z^2 dz = \frac{1}{3} \sum_{l=1}^{nl} (\bar{Q}_{ij})_l (h_l^3 - h_{l-1}^3) \quad (i, j = 1, 2, 6) \quad (20)$$

The coefficients \bar{Q}_{ij} vary from layer to layer and depend on the material properties and the layer orientation α . They are given in Appendix A.

In Eq. (20) h_l is the distance from the median surface to the higher surface of the l th layer. The coefficients \bar{Q}_{ij} may vary from layer to layer.

The transverse displacement w due to the vibration can be written in the form

$$w(\mathbf{x}, t) = w^h(\mathbf{x})e^{\lambda t} \quad (21)$$

in which λ can be decomposed as:

$$\lambda = \sigma + i\omega \quad (22)$$

where σ and ω are the real and imaginary parts of the eigenvalues λ .

b) Free vibration formulation

By substituting Eq. (21) into Eq. (19) and taking a typical term of $w^h(\mathbf{x})$ as $\Phi_j(\mathbf{x})$ and then applying the Galerkin method we have:

$$\begin{aligned} & \sum_{i=1}^{Nod} w_i \iint_{\Omega} [D_{11} \frac{\partial^4 \Phi_i(\mathbf{x})}{\partial x^4} + D_{22} \frac{\partial^4 \Phi_i(\mathbf{x})}{\partial y^4} + 4D_{16} \frac{\partial^4 \Phi_i(\mathbf{x})}{\partial x^3 \partial y} + 4D_{26} \frac{\partial^4 \Phi_i(\mathbf{x})}{\partial x \partial y^3} \\ & + 2(D_{12} + 2D_{66}) \frac{\partial^4 \Phi_i(\mathbf{x})}{\partial x^2 \partial y^2} - (N_x \frac{\partial^2 \Phi_i(\mathbf{x})}{\partial x^2} + 2N_{xy} \frac{\partial^2 \Phi_i(\mathbf{x})}{\partial x \partial y} + N_y \frac{\partial^2 \Phi_i(\mathbf{x})}{\partial y^2}) \\ & \rho h (\frac{\partial^2 \Phi_i(\mathbf{x})}{\partial t^2} + 2v \frac{\partial^2 \Phi_i(\mathbf{x})}{\partial x \partial t} + v^2 \frac{\partial^2 \Phi_i(\mathbf{x})}{\partial x^2})] \Phi_j(\mathbf{x}) dx dy = 0 \end{aligned} \quad (23)$$

Here, $\Phi_j(\mathbf{x})$ is used as typical term of weight functions in the Galerkin method.

The weak form of the Eq. (23) can be represented by

$$\begin{aligned} & \sum_{i=1}^{Nod} w_i \iint_{\Omega} [D_{11} \frac{\partial^2 \Phi_i}{\partial x^2} \frac{\partial^2 \Phi_j}{\partial x^2} + D_{22} \frac{\partial^2 \Phi_i}{\partial y^2} \frac{\partial^2 \Phi_j}{\partial y^2} \\ & + 4D_{16} (\frac{\partial^2 \Phi_i}{\partial x^2} \frac{\partial^2 \Phi_j}{\partial x \partial y} + \frac{\partial^2 \Phi_j}{\partial x^2} \frac{\partial^2 \Phi_i}{\partial x \partial y}) + 4D_{26} (\frac{\partial^2 \Phi_i}{\partial y^2} \frac{\partial^2 \Phi_j}{\partial x \partial y} + \frac{\partial^2 \Phi_j}{\partial y^2} \frac{\partial^2 \Phi_i}{\partial x \partial y}) \\ & + 2D_{12} (\frac{\partial^2 \Phi_i}{\partial x^2} \frac{\partial^2 \Phi_j}{\partial y^2} + \frac{\partial^2 \Phi_j}{\partial x^2} \frac{\partial^2 \Phi_i}{\partial y^2}) + 8D_{66} \frac{\partial^2 \Phi_i}{\partial x \partial y} \frac{\partial^2 \Phi_j}{\partial x \partial y} \\ & + \rho h \lambda^2 \Phi_i \Phi_j + \rho h \lambda v (\frac{\partial \Phi_i}{\partial x} \Phi_j - \frac{\partial \Phi_j}{\partial x} \Phi_i) - \rho h v^2 \frac{\partial \Phi_i}{\partial x} \frac{\partial \Phi_j}{\partial x} \\ & + N_x \frac{\partial \Phi_i}{\partial x} \frac{\partial \Phi_j}{\partial x} + N_{xy} (\frac{\partial \Phi_i}{\partial x} \frac{\partial \Phi_j}{\partial y} + \frac{\partial \Phi_i}{\partial y} \frac{\partial \Phi_j}{\partial x}) + N_y \frac{\partial \Phi_i}{\partial y} \frac{\partial \Phi_j}{\partial y}] dx dy \\ & - \sum_{i=1}^n w_i (\int_{\Gamma} [(\Phi_j V_n - \frac{\partial \Phi_j}{\partial n} M_m) + (N_x n_x \frac{\partial \Phi_i}{\partial x} \Phi_j + N_y n_y \frac{\partial \Phi_i}{\partial y} \Phi_j \\ & + N_{xy} (n_y \frac{\partial \Phi_i}{\partial x} + n_x \frac{\partial \Phi_i}{\partial y}) \Phi_j + \rho h v^2 n_x \frac{\partial \Phi_i}{\partial x} \Phi_j] d\Gamma = 0 \end{aligned} \quad (24)$$

Note that in Eq. (24) M_{nn} and V_n denote the normal moment and shear force on the plate edges, respectively, and $\frac{\partial}{\partial n}$ is partial differentiation with respect to normal direction of plate edge, and moreover, " n_x " and " n_y " are the components of the unit vector normal to the boundary, with Γ symbolizing the boundary.

If the boundary condition is free, M_{nn} and V_n are zero, moreover if the plate edge is simply supported then the normal moment M_{nn} and $w = \sum_{j=1}^{Nod} w_j \Phi_j$ vanish. Also, if the boundary condition is clamped

$w = \sum_{j=1}^{Nod} w_j \Phi_j$ and $\frac{\partial w}{\partial n} = \sum_{j=1}^{Nod} w_j \frac{\partial \Phi_j}{\partial n}$ are enforced to zero. Therefore, the boundary integrals in Eq. (24) disappear when free vibration analysis is of concern.

The matrix form of Eq. (24) can be written as

$$(\lambda^2 \mathbf{M} + \lambda \mathbf{G} + \mathbf{K}) \{\mathbf{w}\} = \{\mathbf{0}\} \quad (25)$$

in which $\{\mathbf{w}\} = \{w_1, w_2, \dots, w_n\}$ is the vector of nodal displacements and \mathbf{M} is the mass matrix in the form of

$$M_{ij} = \iint_{\Omega} \rho h [\Phi_i \Phi_j] dx dy \quad (26)$$

and \mathbf{G} is the gyroscopic matrix of an axially moving plate in the form of

$$G_{ij} = \iint_{\Omega} \rho h v \left[\frac{\partial \Phi_i}{\partial x} \Phi_j - \frac{\partial \Phi_j}{\partial x} \Phi_i \right] dx dy \quad (27)$$

The total stiffness matrix \mathbf{K} in Eq. (25) is

$$\mathbf{K} = \mathbf{k}_b + \mathbf{k}_g^s - \mathbf{k}_g^m \quad (28)$$

where \mathbf{k}_b , \mathbf{k}_g^s and \mathbf{k}_g^m are the bending stiffness matrix, geometric stiffness matrix for a stationary plate and geometric stiffness matrix for a moving plate, respectively. They are:

$$\begin{aligned} [k_b]_{ij} = & \iint_{\Omega} \left[D_{11} \frac{\partial^2 \Phi_i}{\partial x^2} \frac{\partial^2 \Phi_j}{\partial x^2} + D_{22} \frac{\partial^2 \Phi_i}{\partial y^2} \frac{\partial^2 \Phi_j}{\partial y^2} \right. \\ & + 4D_{16} \left(\frac{\partial^2 \Phi_i}{\partial x^2} \frac{\partial^2 \Phi_j}{\partial x \partial y} + \frac{\partial^2 \Phi_j}{\partial x^2} \frac{\partial^2 \Phi_i}{\partial x \partial y} \right) + 4D_{26} \left(\frac{\partial^2 \Phi_i}{\partial y^2} \frac{\partial^2 \Phi_j}{\partial x \partial y} + \frac{\partial^2 \Phi_j}{\partial y^2} \frac{\partial^2 \Phi_i}{\partial x \partial y} \right) \\ & \left. + 2D_{12} \left(\frac{\partial^2 \Phi_i}{\partial x^2} \frac{\partial^2 \Phi_j}{\partial y^2} + \frac{\partial^2 \Phi_j}{\partial x^2} \frac{\partial^2 \Phi_i}{\partial y^2} \right) + 8D_{66} \frac{\partial^2 \Phi_i}{\partial x \partial y} \frac{\partial^2 \Phi_j}{\partial x \partial y} \right] dx dy \end{aligned} \quad (29)$$

$$[k_g^s]_{ij} = \iint [N_x \frac{\partial \Phi_i}{\partial x} \frac{\partial \Phi_j}{\partial x} + N_y \frac{\partial \Phi_i}{\partial y} \frac{\partial \Phi_j}{\partial y} + N_{xy} \left(\frac{\partial \Phi_i}{\partial x} \frac{\partial \Phi_j}{\partial y} + \frac{\partial \Phi_i}{\partial y} \frac{\partial \Phi_j}{\partial x} \right)] dx dy \quad (30)$$

$$[k_g^m]_{ij} = \iint [\rho h v^2 \frac{\partial \Phi_i}{\partial x} \frac{\partial \Phi_j}{\partial x}] dx dy \quad (31)$$

Equation (25) can be rewritten in the following form

$$(\lambda \mathbf{\Theta} + \mathbf{\Lambda}) \{\hat{\mathbf{w}}\} = \{\mathbf{0}\} \quad (32)$$

where

$$\{\hat{\mathbf{w}}\} = \begin{Bmatrix} \lambda \mathbf{w} \\ \mathbf{w} \end{Bmatrix}, \quad \mathbf{\Theta} = \begin{bmatrix} \mathbf{M} & \mathbf{0} \\ \mathbf{0} & \mathbf{k} \end{bmatrix} \quad \text{and} \quad \mathbf{\Lambda} = \begin{bmatrix} \mathbf{G} & \mathbf{k} \\ -\mathbf{k} & \mathbf{0} \end{bmatrix} \quad (33)$$

In the eigenvalue problem (32), $\mathbf{\Theta}$ is a symmetric matrix and $\mathbf{\Lambda}$ is a skew-symmetric one. It should be noted that while all eigenvalues λ are pure imaginary ($\lambda = i\omega$), the traveling plate is stable and the values of ω are the natural frequencies of the plate. When transport speed increases, ω decreases until at a certain critical speed, the first natural frequency of the system becomes zero. For speeds higher than the critical speed, the plate may experience flutter instability as in unstable conditions the real part of at least one of the eigenvalues λ is non-zero ($\sigma \neq 0$) [1].

4. PLATE PROPERTIES AND BOUNDARY CONDITIONS

a) Shape of plates

Figure 1 shows a plate moving between two bilateral rollers, one of which is along the y -axis at $x=0$ and the skew angle of the second one is β . Although in many practical applications the longitudinal edges are free, various boundary conditions are considered in this research. The in-plane tension in x -direction may be non-uniform and vary linearly.

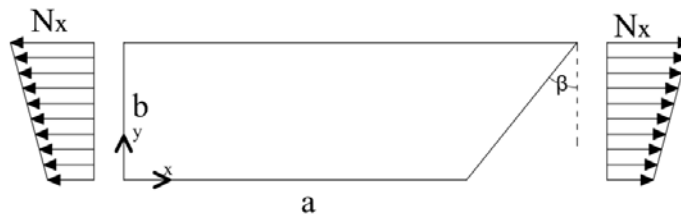


Fig. 1. An axially moving plate between two rollers

In some practical applications, moving plates pass over intermediate rollers or supports which may be modeled in the form of line supports which are assumed to be frictionless. The out-of-plane displacement for nodes located along line supports vanishes (see Fig. 2).

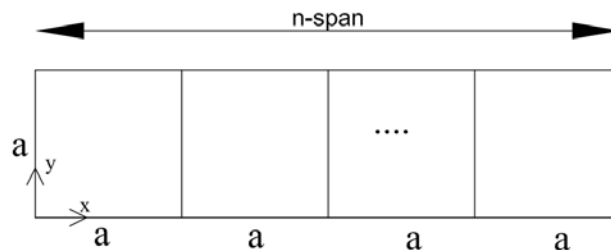


Fig. 2. A multi-span moving plate

b) Material of laminated moving plate

One layer orthotropic plate, five-layer symmetrically angle-ply, and three-layer cross-ply laminated plates are examined in the numerical results. The cross-ply laminates considered have lay-up $[0^\circ/90^\circ/0^\circ]$ with the dimensionless orthotropic material properties of $E_1/E_2=40$ and $G_{12}/E_2=0.6$, $\nu_{12}=0.25$ as chosen by Leung and Zhou [32].

The lay-up of five-layer angle-ply plates, which have been used by Chow et al [33], is $[\alpha/-\alpha/\alpha/-\alpha/\alpha]$ with $\alpha=0^\circ, 15^\circ, 30^\circ, 45^\circ$. The material properties are $E_1/E_2=15.4$, $G_{12}/E_2=0.79$, $\nu_{12}=0.3$. It should be noted that, for the case of $\alpha=0$ the plate is regular orthotropic.

c) Essential boundary conditions

The use of MLS approximation produces shape functions which do not possess the Kronecker delta function property, i.e. $\Phi_i(x_j) \neq \delta_{ij}$. It implies that the essential boundary conditions cannot be imposed in the same way as in the conventional finite element method. The essential boundary conditions are satisfied by using Lagrange multipliers in the following weak form equation [26]

$$\int_{S_w} \delta \lambda^T (\hat{w} - \bar{w}) ds = 0 \quad (34)$$

where λ is a vector of Lagrange multiplier, \bar{w} is the prescribed essential boundary conditions and \hat{w} denotes the deflection and rotation about the tangent to the boundary.

The discrete form of the essential boundary conditions derived from Eq. (34) can be written as

$$[\mathbf{H}]_{2nb \times n} \{\mathbf{w}\}_{n \times 1} = \{\mathbf{0}\} \quad (35)$$

where nb is the number of constraint points on the boundary. For a clamped boundary, H_{ij} may be expressed as

$$H_{ij} = \int_{S_w} [N_i \Phi_j \ N_i \Phi_{j,n}]^T ds \quad (36)$$

and for a simply supported boundary it is given by

$$H_{ij} = \int_{S_w} [N_i \Phi_j \ 0]^T ds \quad (37)$$

Here N_i is a Lagrange interpolation function along the boundaries, and n in Eq. (36) is the unit normal to the boundary. Generally, the matrix \mathbf{H} is sparse and singular. Using singular-value decomposition technique, it can be decomposed as

$$\mathbf{H}_{2nb \times n} = \mathbf{R}_{2nb \times 2nb} \begin{bmatrix} \Sigma_{r \times r} & \mathbf{0} \\ \mathbf{0} & \mathbf{0} \end{bmatrix}_{2nb \times n} \mathbf{V}_{n \times n}^T \quad (38)$$

where \mathbf{R} and \mathbf{V} are the orthogonal matrices, Σ is the singular value of \mathbf{H} , and r is the rank of \mathbf{H} , which represents the number of independent constraints.

The matrix \mathbf{V} can be written as

$$\mathbf{V}^T = \{\mathbf{V}_{n \times r} \ \mathbf{V}_{n \times (n-r)}\}^T \quad (39)$$

Performing orthogonal transformation in Eq. (32), the eigenvalue equation can be expressed as

$$(\lambda \tilde{\mathbf{\Theta}} + \tilde{\mathbf{\Lambda}}) \{\tilde{\mathbf{O}}\} = \{\mathbf{0}\} \quad (40)$$

where

$$\tilde{\mathbf{\Theta}} = \begin{bmatrix} \tilde{\mathbf{M}} & \mathbf{0} \\ \mathbf{0} & \tilde{\mathbf{k}} \end{bmatrix} \quad \text{and} \quad \tilde{\mathbf{\Lambda}} = \begin{bmatrix} \tilde{\mathbf{G}} & \tilde{\mathbf{k}} \\ -\tilde{\mathbf{k}} & \mathbf{0} \end{bmatrix} \quad (41)$$

in which

$$\tilde{\mathbf{k}} = \mathbf{V}_{(n-r) \times n}^T \mathbf{k} \mathbf{V}_{n \times (n-r)}, \quad \tilde{\mathbf{G}} = \mathbf{V}_{(n-r) \times n}^T \mathbf{G} \mathbf{V}_{n \times (n-r)}, \quad \tilde{\mathbf{M}} = \mathbf{V}_{(n-r) \times n}^T \mathbf{M} \mathbf{V}_{n \times (n-r)} \quad (42)$$

and $\tilde{\mathbf{O}}$ is matrix of eigenvectors. Solution of Eq. (40) gives the natural frequency of plate free vibration.

5. RESULTS AND DISCUSSIONS

a) General

Non-dimensional variables used in the results are expressed as

$$\Omega = \omega \frac{b^2}{2\pi^2} \sqrt{\frac{\rho h}{D_o}}, \quad c^2 = v^2 \frac{b^2 \rho h}{\pi^2 D_o}, \quad r = \frac{a}{b}, \quad (k_x, k_y) = (N_x, N_y) \frac{b^2}{\pi^2 D_o} \quad (43)$$

where Ω and c denote dimensionless natural frequency and traveling speed, respectively. k_x and k_y are in-plane load parameters along x - and y -directions, respectively (positive when tensile) and finally, r is aspect ratio of the plate. The stiffness parameter D_o in Eq. (43) is defined as

$$D_o = \frac{E_2 h^3}{12(1 - \nu_{12} \nu_{21})} \quad (44)$$

In all tables, S denotes simply supported while C and F mean clamped and free boundary conditions, respectively. For instance, notation SFSF means that the left and right edges of the plate are simply supported while the upper and lower edges are free.

b) Validity and convergence study

The numerical procedure based on the EFG method presented in this paper has been implemented in MATLAB and applied to axially moving laminated composite plates.

The convergence study using the EFG method with regular distributed nodes is presented in Table 1 for a SFSF axially moving cross-ply laminated plate. The aspect ratio of the plate and skew angle of end roller are 1.3 and 0° , respectively. Normalized axial force k_x varies linearly along plate width from 10.0 to 20.0. The obtained results for two different axial speeds are compared with those obtained by Hatami et al [1].

Table 1. Frequency parameters Ω for the axially moving SFSF cross-ply laminated plate subjected to non-uniform axial tension ($\beta=0$)

EFG nodes	c=1			c=4		
	Ω_1	Ω_2	Ω_3	Ω_1	Ω_2	Ω_3
4×4	2.4724	2.8048	3.7605	1.9070	2.2952	3.3081
5×5	2.2856	2.4927	3.3122	1.6780	1.9391	2.8771
6×6	2.2693	2.4699	3.2841	1.6199	1.8685	2.7915
7×7	2.2663	2.4676	3.2584	1.6117	1.8605	2.7469
8×8	2.2673	2.4677	3.2311	1.6135	1.8614	2.7208
9×9	2.2677	2.4671	3.2250	1.6140	1.8607	2.7138
10×10	2.2754	2.4747	3.2310	1.6214	1.8674	2.7181
11×11	2.2622	2.4614	3.2159	1.6076	1.8543	2.7026
Ref [1]	2.2648	2.4648	3.2243	1.6092	1.8562	2.7105

From the convergence study carried out in Table 1, we find that when an 11×11 nodal density is used, the present results have a good agreement with the previous study.

The results show that the rate of convergence for higher axial speed is lower, mainly because axial velocity leads to complex modes and the amount of the complexity grows with the increase of axial speed.

The ability of the EFG method in modeling of angle-ply laminates and intermediate supports is shown in Table 2 by comparing the results with those obtained by Cheung and Zhou [34] and Hatami et al [1]. In Table 2 the first six frequency parameters of a symmetric angle-ply laminated plate with three equal spans (n-span= 3) as shown in Fig. 2, are given. The plate is simply supported at all edges and the orientation of the major direction is $\alpha=45^\circ$. The results are for stationary condition ($v=0$). The results obtained by using the EFG method are in good agreement with the previous studies.

Table 2. First six frequency parameters Ω for a stationary three-span angle-ply laminated plate with simply supported edges ($\beta=0$)

EFG nodes	c=0					
	Ω_1	Ω_2	Ω_3	Ω_4	Ω_5	Ω_6
Present method	2.75	2.89	3.35	5.83	6.14	6.43
Ref. [34]	2.80	2.95	3.35	5.81	6.11	6.40
Ref [1]	2.80	2.94	3.39	5.79	6.12	6.40

The first six frequency parameters for an orthotropic four-span plate with different orthotropicity ratio (E_1/E_2) are listed in Table 3 and compared with obtained results by using the finite strip method that was carried out by Hatami et al[1]. The non-dimensional speed variable c is equal to 2 and normalized axial force k_x is constant along plate width ($k_x=2$). A good agreement between the two methods is observed.

Table 3. First six frequency parameters Ω for a moving orthotropic four-span plate with simply supported edges ($\beta=0$)

Mode	Present method			Ref [1]		
	$E_1/E_2=1$	$E_1/E_2=10$	$E_1/E_2=20$	$E_1/E_2=1$	$E_1/E_2=10$	$E_1/E_2=20$
1	0.5423	1.6143	2.2635	0.5332	1.6067	2.2552
2	0.5978	1.8662	2.6306	0.5864	1.8531	2.6151
3	0.7466	2.4847	3.2624	0.7284	2.4510	3.2028
4	0.9181	2.8212	3.5243	0.9071	2.7575	3.4777
5	2.1493	2.9905	3.5419	2.0701	2.9229	3.4795
6	2.1863	3.1608	4.2710	2.1013	3.1512	4.1916

c) Numerical studies for straight-end roller

First six frequency parameters for a rectangular cross-ply laminated plate with $r=1.3$ and different boundary conditions are shown in Tables 4 to 6. The plate is subjected to a non-uniformly distributed axial tension load varying linearly along the plate width from $kx=10$ to $kx=20$. The obtained results are presented for different axial velocity parameters c .

Table 4. First six frequency parameters Ω for a moving cross-ply laminated plate with SFSF edges

Mode	Ω				
	$c=1$	$c=2$	$c=3$	$c=4$	$c=5$
1	2.2622	2.1379	1.9246	1.6076	1.1424
2	2.4614	2.3444	2.1451	1.8543	1.4475
3	3.2159	3.1141	2.9436	2.7026	2.3873
4	5.7969	5.7047	5.5517	5.3386	5.0663
5	7.8470	7.7508	7.5885	7.3569	7.0510
6	8.0798	7.9847	7.8245	7.5962	7.2955

Table 5. First six frequency parameters Ω for a moving cross-ply laminated plate with CFCF edges

Mode	Ω				
	$c=1$	$c=2$	$c=3$	$c=4$	$c=5$
1	4.4265	4.3283	4.1646	3.9349	3.9349
2	4.5562	4.4600	4.2997	4.0749	4.0749
3	5.0371	4.9446	4.7906	4.5753	4.5753
4	7.0010	6.9126	6.7658	6.5615	6.5615
5	11.3820	11.2880	11.1320	10.9150	10.9150
6	11.8970	11.8250	11.7040	11.5330	11.5330

Table 6. First six frequency parameters Ω for a moving cross-ply laminated plate with SSSS edges

Mode	Ω				
	$c=1$	$c=2$	$c=3$	$c=4$	$c=5$
1	2.5371	2.4215	2.2252	1.9405	1.5479
2	4.1129	4.0166	3.8563	3.6322	3.3444
3	7.7101	7.6087	7.4410	7.2085	6.9132
4	8.0561	7.9613	7.8014	7.5738	7.2741
5	8.9096	8.8234	8.6785	8.4731	8.2045
6	11.3590	11.2940	11.1840	11.0270	10.8200

For rectangular moving angle-ply laminated plates with line supports shown in Fig. 2, the first six frequency parameters are presented in Tables 7 to 9. For various boundary conditions, the critical speeds, in which one of the natural frequencies of plate vanishes, are presented. The orientation of the major direction is $\alpha=45^\circ$ and $\beta=0$.

Table 7. First six frequency parameters Ω for a moving angle-ply laminated two-span plate

Mode	SSSS		CFCF		SFSF	
	$c_{cr}=5.4040$		$c_{cr}=2.9058$		$c_{cr}=1.9941$	
	$c=0$	$c=0.5c_{cr}$	$c=0$	$c=0.5c_{cr}$	$c=0$	$c=0.5c_{cr}$
1	2.7263	2.1390	1.6018	1.3322	0.9977	0.8420
2	3.0715	2.4806	2.3404	2.1177	1.5166	1.3899
3	5.6919	5.1687	2.7777	2.5926	2.3564	2.2672
4	6.1022	5.6832	3.1634	2.9869	2.4916	2.4027
5	7.1080	6.5980	5.3476	5.1922	4.2922	4.1956
6	7.4523	6.8548	5.3591	5.2117	4.5900	4.5163

Table 8. First six frequency parameters Ω for a moving angle-ply laminated three-span plate

Mode	SSSS		CFCF		SFSF	
	$c_{cr}=5.4564$		$c_{cr}=2.5065$		$c_{cr}=2.004$	
	$c=0$	$c=0.5c_{cr}$	$c=0$	$c=0.5c_{cr}$	$c=0$	$c=0.5c_{cr}$
1	2.7523	2.1662	1.3126	1.0996	1.0022	0.8469
2	2.8856	2.2995	1.9261	1.7514	1.2670	1.1298
3	3.3470	2.7472	2.3593	2.1968	1.8493	1.7344
4	5.8258	5.3962	2.5927	2.4587	2.3338	2.2476
5	6.1350	5.8153	3.0007	2.8731	2.5068	2.4170
6	6.4284	6.0782	3.1639	3.0378	2.7928	2.7058

Table 9. First six frequency parameters Ω for a moving angle-ply laminated four-span plate

Mode	SSSS		CFCF		SFSF	
	$c_{cr}=5.5325$		$c_{cr}=2.3420$		$c_{cr}=2.0595$	
	$c=0$	$c=0.5c_{cr}$	$c=0$	$c=0.5c_{cr}$	$c=0$	$c=0.5c_{cr}$
1	2.7888	2.2104	1.2026	1.0130	1.0305	0.8740
2	2.8544	2.3006	1.6042	1.4475	1.1832	1.0437
3	3.1560	2.6348	2.1206	1.9798	1.5685	1.4382
4	3.4994	2.9807	2.3843	2.2710	2.0161	1.9025
5	6.1756	5.8223	2.5500	2.4380	2.4013	2.3126
6	6.5094	6.1732	2.8344	2.7374	2.4424	2.3663

For a moving angle-ply laminated plate with $\alpha=45^\circ$ subjected to a uniform axial tension, the variation of the fundamental frequency parameter Ω_1 against transport speed parameter c is given in Fig. 3.

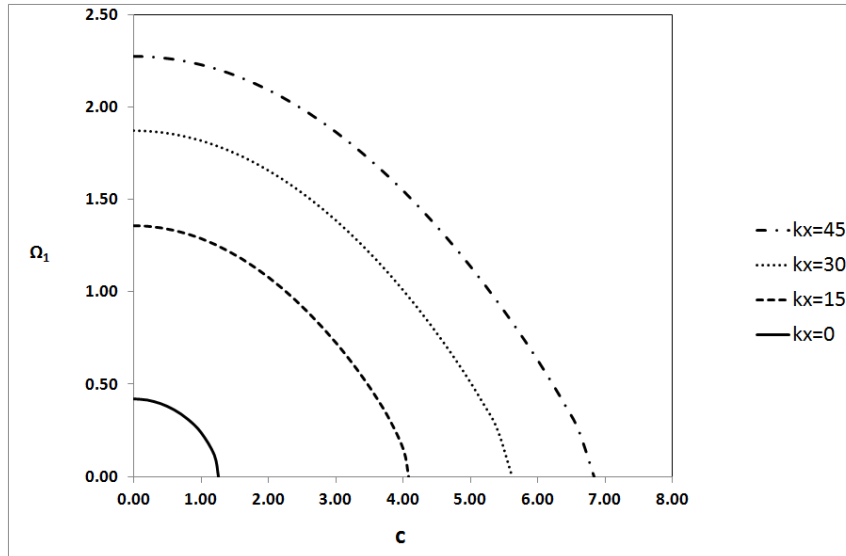


Fig. 3. The effect of axial speed on the fundamental frequency of a SFSF angle-ply one-span plate

The plate boundary is SFSF and is single-span with aspect ratio $r=1.5$. As shown in the figure, the natural frequency decreases when the axial speed increases till the speed reaches its critical value, at which natural frequency becomes zero. As shown in Fig. 3, for a certain speed, the fundamental frequency has greater values for larger in-plane tensions, because based on the Eqs. (28) and (30), the stiffness of the plate increases by increasing of in-plane tensions.

For a constant axial velocity ($c=4.0$) and axial tension ($k_x=15$), the variation of Ω_1 against aspect ratio r of the cross-ply laminated plate is given in Fig. 4. Three types of boundary conditions SFSF, CFCF and SSSS are considered. The natural frequency decreases rapidly when the aspect ratio increases. It can also be seen that the natural frequency of SSSS moving plate with $r>3$ is higher than CFCF and SFSF ones.

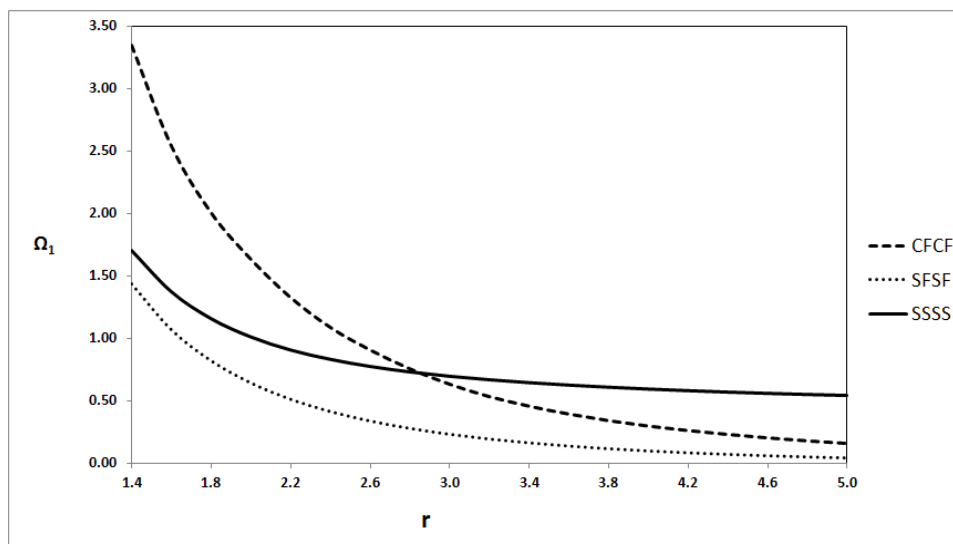


Fig. 4. Variation of the first frequency parameter against the aspect ratio for a moving one-span cross-ply plate

The six first mode shapes of a rectangular cross-ply laminated plate with SSSS boundary conditions are shown in Fig. 5.

d) Numerical studies for skew-end roller

In spite of wide appearance of skew rollers in some of moving systems such as power transmission belts, lines of composite sheets production and conveyor belts, the authors have not found any information on the vibration of these axially moving plates in the open literature. Hatami et al, performed nonlinear analysis of axially moving plates using the finite element method [35]. They considered the effect of skew-end roller in their research.

Free vibration of axially moving plate with skew-end roller shown in Fig. 2, is analyzed using the EFG method for an angle-ply laminated SFSF plate. The natural frequencies of the first six modes are shown in Table 10 for stationary plate and moving one. The aspect ratio of the plate a/b is 1.5, and the plate is subjected to uniform axial tension ($k_x=10$). The results are presented for various values of fiber orientations α .

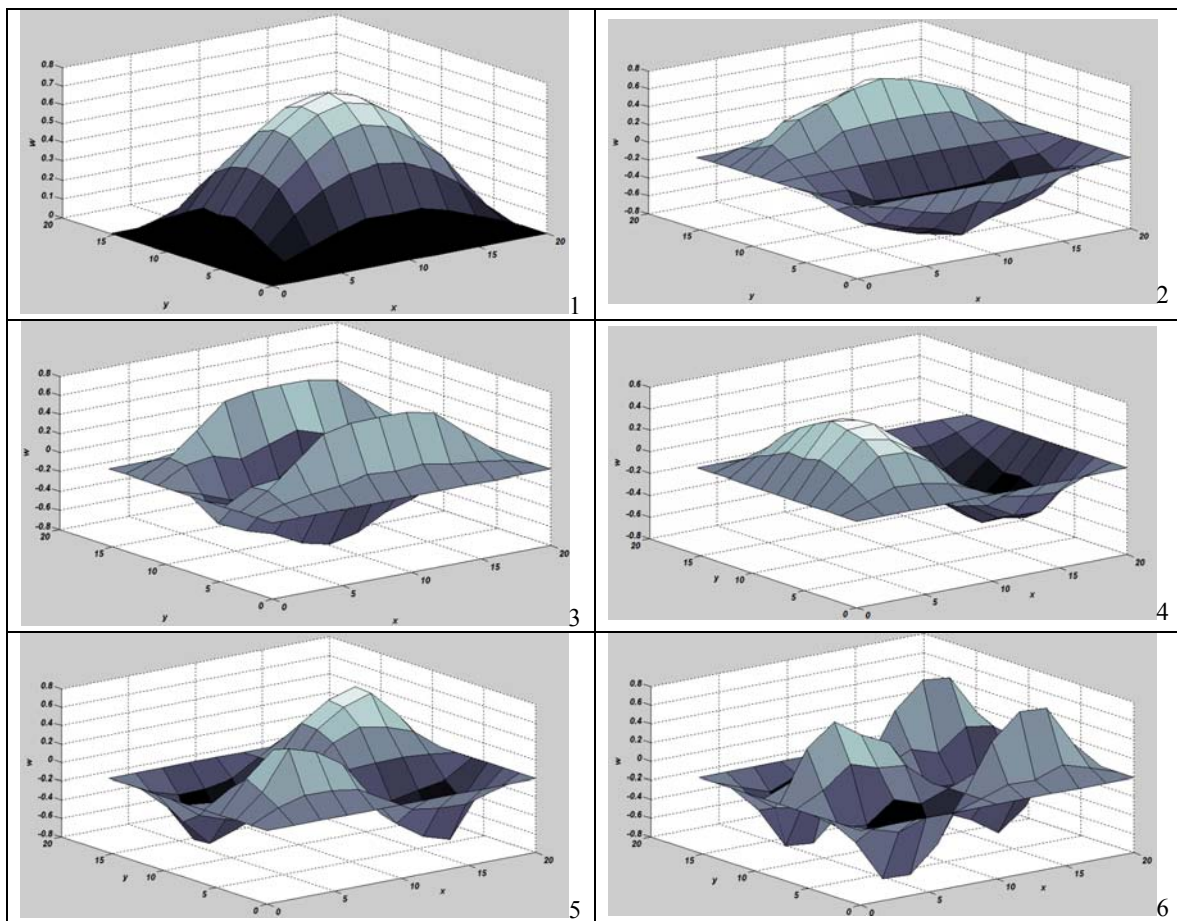


Fig. 5. Six first mode shapes for a moving one-span cross-ply plate

For a moving SFSF cross-ply laminated plate with $c=3$, the effect of uniform axial force on the fundamental frequency of the plate for various skew angles can be observed in Fig. 6. The plate aspect ratio is $a/b=1.5$ and the critical axial force, shown in the figure, is the minimum axial force required for the plate stability.

Table 10. First six frequency parameters Ω for a moving angle-ply laminated skew end plate with ($\beta=30$)

Mode	$\alpha=0$		$\alpha=15$		$\alpha=30$		$\alpha=45$	
	$c=0$	$c=2$	$c=0$	$c=2$	$c=0$	$c=2$	$c=0$	$c=2$
1	0.9953	0.7978	0.9699	0.7575	0.9245	0.6850	0.8926	0.6229
2	1.3307	1.1297	1.3766	1.1755	1.4800	1.2751	1.4775	1.2428
3	2.0003	1.8394	2.2811	2.1313	2.2780	2.0158	2.0620	1.7463
4	2.6831	2.4910	2.5330	2.3204	2.8467	2.7029	3.1450	2.7974
5	3.5032	3.3181	3.4823	3.2689	3.4079	3.1700	3.4456	3.2755
6	3.7185	3.5634	4.1728	4.0476	4.2561	4.0137	3.7275	3.4798

For a constant axial tension ($k_x=10$), the variation of Ω_1 against axial speed parameter c for different values of skew angle β of the cross-ply SFSF laminated plate is given in Fig. 7. The natural frequency decreases rapidly when the axial speed increases, as shown in the figure.

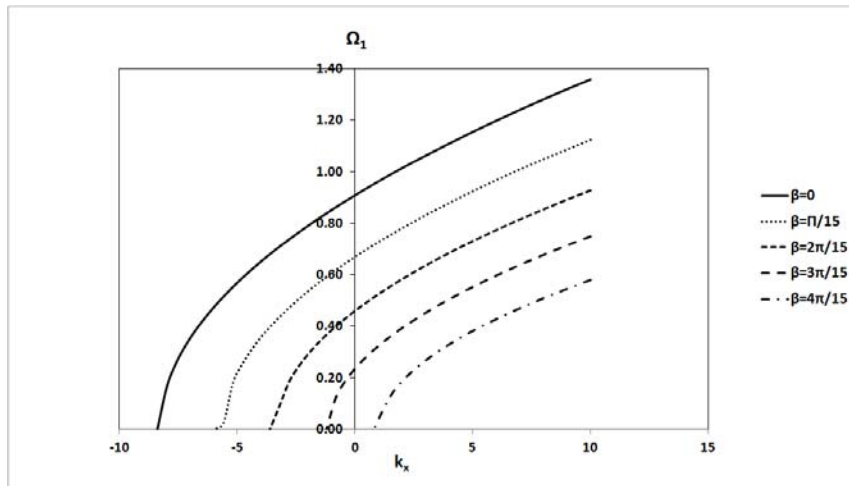


Fig. 6. Variation of the first frequency parameter against the axial uniform load for a moving skew-end cross-ply plate

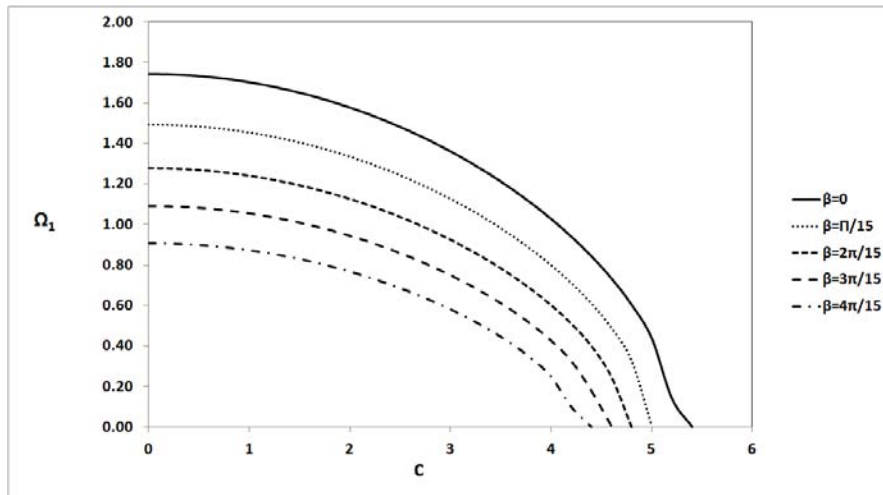


Fig. 7. Variation of the first frequency parameter against the axial speed for a moving skew-end cross-ply plate

6. CONCLUSION

An element-free Galerkin (EFG) formulation is employed to study the free vibration of laminated composite plates. Numerical results for skew-end roller and axially moving plates with intermediate line supports are presented. Some numerical experiments are carried out, to illustrate the ability and efficiency of the method and also to examine the effects of some parameters such as layers orientation, aspect ratio, axial speed, in-plane forces, and line supports on the natural frequencies of moving laminated plates.

Generally, natural frequency of moving laminated plates increases by decreasing the axial speed of plate and aspect ratio while it decreases by increasing of in-plane axial tension.

For plates with skew-end roller, with decrease of skew angle, an increase in natural frequency of plate is observed.

This research shows that the EFG method is computationally efficient, moreover, it is a very simple procedure for modeling the skew plates with various boundary conditions.

REFERENCES

1. Hatami, S., Azhari, M. & Saadatpour, M. M. (2007). Free vibration of moving laminated composite plates. *Compos. Struct.*, Vol. 80, No. 4, pp. 609-620.
2. Pellicano, F. & Vestroni, F. (2000). Nonlinear dynamics and bifurcations of an axially moving beam. *J. Vib. Acoust.*, Vol. 122, pp. 21-30.
3. Ashley, H. & Haviland, G. (1950). Bending vibrations of a pipe line containing flowing fluid. *J. Appl. Mech.* Vol. 17, pp. 229-232.
4. Swope, R. D. & Ames, W. F. (1963). Vibrations of moving threadline. *J. the Franklin Institute*, Vol. 275, pp. 36-55.
5. Mote, C. D. (1965). A study of band saw vibrations. *J. the Franklin Institute*, Vol. 279, pp. 430-444.
6. Simpson, A. (1973). Transverse modes and frequencies of beams translating between fixed end supports. *J. Mech. Eng. Sci.*, Vol. 15, No. 3, pp. 159-164.
7. Ulsoy, A. G. & Mote, C. D. (1982). Vibration of wide band saw blades. *J. Eng. Ind.*, Vol. 104, pp. 71-78.
8. Lin, C. C. & Mote, C. D. (1995). Equilibrium displacement and stress distribution in a two dimensional, axially moving web under transverse loading. *J. Appl. Mech.*, Vol. 62, No. 3, pp. 772-779.
9. Lengoca, L. & McCallion, H. (1995). Wide bandsaw blade under cutting conditions: Part I: Vibration of a plate moving in its plane while subjected to tangential edge loading. *J. Sound Vib.*, Vol. 186, No. 1, pp. 125-142.
10. Lin, C. C. (1997). Stability and vibration characteristics of axially moving plates. *Int. J. Solids Struct.*, Vol. 34, No. 24, pp. 3179-3190.
11. Wang, X. (1999). Numerical analysis of moving orthotropic thin plates, *Comput. Struct.*, Vol. 70, No. 4, pp. 467-486.
12. Laukkanen, J. (2002). FEM analysis of a travelling web. *Comput. Struct.*, Vol. 80, No. 24, pp. 1827-1842.
13. Luo, Z. & Hutton, S. G. (2002). Formulation of a three-node traveling triangular plate element subjected to gyroscopic and in-plane forces. *Comput. Struct.*, Vol. 80, No. 26, pp. 1935-1944.
14. Hatami, S., Ronagh, H. R. & Azhari, M. (2008). Exact free vibration analysis of axially moving viscoelastic plates. *Comput. Struct.*, Vol. 86, No. 17-18, pp. 1738-1746.
15. Wang, L., Hu, Z. & Zhong, Z. (2010). Dynamic analysis of an axially translating plate with time-variant length. *Acta Mecha.*, Vol. 215, No. 1-4, pp. 9-23.
16. Binesh, S. M., Hataf, N. & Ghahramani, A. (2007). Elastic analysis of reinforced soils using point interpolation method. *Iranian Journal of Science & Technology, Transaction B, Engineering*, Vol. 31, No. B5, pp. 577-581.

17. Javanmard, S. A. S., Daneshmand, F., Moshksar, M. M. & Ebrahimi, R. (2011). Meshless analysis of backward extrusion by natural element method. *Iranian Journal of Science & Technology, Transaction B, Engineering*, Vol. 35, No. M2, pp 167-180.
18. Zheng, B. & Dai, B. (2011). A meshless local moving Kriging method for two-dimensional solids. *Appl. Math. Comput.*, Vol. 218, No. 2, pp. 5113–5124.
19. Monaghan, J. J. (1998). An introduction to SPH. *Comput. Phys. Commun.* Vol. 48, No. 1, pp. 89–96.
20. Atluri, S. N. & Zhu, T. (1998). A new Meshless Local Petrov-Galerkin (MLPG) approach in computational mechanics. *Comput. Mech.*, Vol. 22, pp. 117-127.
21. Oñate, E., Idelsohn, S., Zienkiewicz, O. C. & Taylor, R. L. (1996). A finite point method in computational mechanics. A application to convective transport and fluid flow. *Int. J. Numer. Meth. Eng.*, Vol. 39, No. 22, pp. 3839-3866.
22. Oñate, E., Idelsohn, S., Zienkiewicz, O. C., Taylor, R. L. & Sacco, C. (1996). A stabilized finite point method for analysis of fluid mechanics problems. *Comput. Meth. Appl. Mech. Eng.*, Vol. 139, No. 1-4, pp. 315-346.
23. Oñate, E. & Idelsohn, S. (1988). A mesh-free finite point method for advective-diffusive transport and fluid flow problems. *Comput. Mech.*, Vol. 21, No. 4-5, pp. 283-292.
24. Belytschko, T., Lu, Y. Y. & Gu, L. (1994). Element-free Galerkin methods. *Int. J. Numer. Meth. Eng.*, Vol. 37, No. 2, pp. 229–256.
25. Belytschko, T., Krongauz, Y., Organ, Y. D., Fleming, M. & Krysl, P. (1996). Meshless methods: an overview and recent developments. *Comput. Metod Appl. M.*, Vol. 139, No. 1-4, pp. 3–47.
26. Liu, G. R., Chen, X. L. & Reddy J. N. (2002). Buckling of symmetrically laminated composite plates using the element-free Galerkin method. *Int. J. Struct. Stab. Dyn.*, Vol. 2, No. 3, pp. 281-294.
27. Krysl, P. & Belytschko, T. (1995). Analysis of thin plates by the element-free Galerkin method. *Comput. Mech.*, Vol. 17, No. 1-2, pp. 26-35.
28. Krysl, P. & Belytschko, T. (1996). Analysis of thin shells by the element-free Galerkin method. *Int. J. Solids Struct.*, Vol. 33, No. 20-22, pp. 3057–3080.
29. Belinha, J. & Dinis, L. M. J. S. (2007). Nonlinear analysis of plates and laminates using the element free Galerkin method. *Compos. Struct.*, Vol. 78, No. 3, pp. 337-350.
30. Belinha, J. & Dinis, L. M. J. S. (2007). Analysis of plates and laminates using the element-free Galerkin method. *Comput. Struct.*, Vol. 84, No. 22-23, pp. 1547–1559.
31. Liu, G. R. (2003). *Mesh free methods*. CRC Press, New York.
32. Leung, A. Y. T. & Zhou, W. E. (1996). Dynamic stiffness analysis of laminated composite plates. *Thin Wall. Struct.*, Vol. 25, No. 2, pp. 109-133.
33. Chow, S. T., Liew, K. M. & Lam, K. Y. (1992). Transverse vibration of symmetrically laminated rectangular composite plates. *Compos. Struct.*, Vol. 20, No. 4, pp. 213-226.
34. Cheung, Y. K. & Zhou, D. (2001). Vibration analysis of symmetrically laminated rectangular plates with intermediate line supports. *Comput. Struct.*, Vol. 79, No. 1, pp. 33-41.
35. Hatami, S., Azhari, M. & Saadatpour, M. M. (2007). Nonlinear analysis of axially moving plates using FEM. *Int. J. Struct. Stab. Dyn.*, Vol. 7, No. 4, pp. 589-607.

APPENDIX A: \bar{Q}_{ij} coefficients

$$\bar{Q}_{11} = Q_{11} \cos^4 \alpha + 2(Q_{12} + 2Q_{66}) \sin^2 \alpha \cos^2 \alpha + Q_{22} \sin^4 \alpha \quad (\text{A.1})$$

$$\bar{Q}_{12} = (Q_{11} + Q_{22} - 4Q_{66}) \sin^2 \alpha \cos^2 \alpha + Q_{12} (\sin^4 \alpha + \cos^4 \alpha) \quad (\text{A.2})$$

$$\bar{Q}_{16} = (Q_{11} - Q_{12} - 2Q_{66}) \sin \alpha \cos^3 \alpha + (Q_{12} - Q_{22} + 2Q_{66}) \sin^3 \alpha \cos \alpha \quad (\text{A.3})$$

$$\bar{Q}_{22} = Q_{11} \sin^4 \alpha + 2(Q_{12} + 2Q_{66}) \sin^2 \alpha \cos^2 \alpha + Q_{22} \cos^4 \alpha \quad (\text{A.4})$$

$$\bar{Q}_{26} = (Q_{11} - Q_{12} - 2Q_{66}) \sin^3 \alpha \cos \alpha + (Q_{12} - Q_{22} + 2Q_{66}) \sin \alpha \cos^3 \alpha \quad (\text{A.5})$$

$$\bar{Q}_{66} = (Q_{11} + Q_{22} - 2Q_{12} - 2Q_{66}) \sin^2 \alpha \cos^2 \alpha + Q_{66} (\sin^4 \alpha + \cos^4 \alpha) \quad (\text{A.6})$$

$$Q_{11} = \frac{E_1}{1 - \nu_{12}\nu_{21}} \quad (\text{A.7})$$

$$Q_{12} = \frac{\nu_{12}E_2}{1 - \nu_{12}\nu_{21}} \quad (\text{A.8})$$

$$Q_{22} = \frac{E_2}{1 - \nu_{12}\nu_{21}} \quad (\text{A.9})$$

$$Q_{66} = G_{12} \quad (\text{A.10})$$

$$\frac{\nu_{12}}{\nu_{21}} = \frac{E_1}{E_2} \quad (\text{A.11})$$

where E_1 and E_2 denote the Young's moduli parallel to and perpendicular to the fibers while ν_{12} and ν_{21} are the corresponding Poisson's ratios; α is the anticlockwise angle of fiber orientation of a layer from the positive x -direction. G_{12} is the shear modulus of laminates.